

RESEARCH ARTICLE OPEN ACCESS

Anastomosis and Low Flows Sustain Resilient Groundwater Dependent Riparian Floodplains in an Agricultural River Valley, New Mexico

Ellen Soles¹ | Martha Cooper² | Laurel Saito³ 

¹Colorado Plateau Cooperative Ecosystems Study Unit, Northern Arizona University, Flagstaff, Arizona, USA | ²The Nature Conservancy in New Mexico, Santa Fe, New Mexico, USA | ³The Nature Conservancy in Nevada, Reno, Nevada, USA

Correspondence: Laurel Saito (laurel.saito@tnc.org)

Received: 26 May 2025 | **Revised:** 10 December 2025 | **Accepted:** 7 January 2026

Keywords: anastomosis | Colorado River basin | connectivity | ecosystem resilience | Gila River | groundwater dependent ecosystems | long-term datasets | natural flow regime

ABSTRACT

In arid regions with limited water supplies like the Colorado River basin of the southwestern United States, flow regimes and water availability are major controls on native riparian ecosystems' resilience, persistence and function. In this paper, we share a case study that uses a long-term dataset of topographic, vegetation and groundwater data collected over water years 2011–2021 to demonstrate how secondary channels formed during high flow events enhance groundwater-dependent riparian ecosystem resilience, favouring native over non-native vegetation. In the Cliff-Gila Valley of southwestern New Mexico, channelization and levee construction between 1940 and 1980 profoundly altered the floodplain and channel of the Gila River, a Colorado River tributary. During subsequent large floods, river anastomosis (branching) left a network of secondary channels across the floodplain. Long-term data show that these channels improve vegetation access to groundwater, facilitating regeneration and expansion of diverse native groundwater-dependent vegetation. Data also show that even the lowest perennial flows ($0.4\text{--}0.6\text{ m}^3\text{ s}^{-1}$) sustain rates of groundwater recession favourable to successful native riparian seedling recruitment in the topographic lows created by secondary channels. Alluvial groundwater recedes more sharply in a reach seasonally dewatered by irrigation diversions, but seepage through diversion structures and unlined ditches maintains shallow groundwater levels. This case study demonstrates that even in arid regions, robust native groundwater-dependent riparian areas can co-exist with human water demands when large floods can move across broad floodplains and create topographic complexity. The study also highlights the importance of long-term datasets for documenting ecosystem resilience to floods, drought and ongoing climate change.

1 | Introduction

In semi-arid regions, many native riparian habitats are groundwater-dependent ecosystems (GDEs), in which groundwater availability forms a major control on ecosystem resilience and function (Lite and Stromberg 2005; Mayes et al. 2020; Rohde et al. 2021; Rood, Braatne, et al. 2003). These ecosystems can contribute significantly to regional biodiversity, comprising unique assemblages distinct from those of surrounding uplands (Kauffman and Krueger 1984; Patten 1998;

Sabo et al. 2005; Van der Nat et al. 2003; Whited et al. 2007). Across the Northern hemisphere, *Salicaceae* (cottonwood/willow) woodlands provide essential foundations for these ecosystems (Ellison et al. 2005; Gitlin et al. 2006; Gonzalez et al. 2018; Rood et al. 2010), creating complex, multi-height canopy cover and an ecologically diverse mosaic of habitats across floodplains and adjacent terraces (Kondolf 2011; Merritt and Bateman 2012). Despite occupying a relatively small spatial area, riparian zones therefore support large percentages of mammals, birds, reptiles and amphibians in the arid Western

This is an open access article under the terms of the [Creative Commons Attribution-NonCommercial](https://creativecommons.org/licenses/by-nc/4.0/) License, which permits use, distribution and reproduction in any medium, provided the original work is properly cited and is not used for commercial purposes.

© 2026 The Author(s). *Hydrological Processes* published by John Wiley & Sons Ltd.

United States (Fernald et al. 2007), while sustaining human well-being with materials, recreation, water quality improvements and other ecosystem services (Dufour et al. 2019).

However, native riparian GDEs can also be highly vulnerable to extended drought and other impacts resulting from climate change, water extraction and human alteration of the landscape (Capon et al. 2013; NRC 2002; Wohl et al. 2021), which stress the hydrologic dynamics connecting surface flows and shallow groundwater (Mayes et al. 2020). In many arid land riparian systems, flow regulation is a major factor in reducing their resilience to changes in climate and water availability (Rohde et al. 2021), thus shifting these native riparian forests towards non-native species (Horton and Clark 2001; Merritt and Poff 2010; Stromberg, Lite, et al. 2007). In addition, persistent drought has afflicted the southwestern United States in recent decades (Williams et al. 2022), particularly in the Colorado River basin of the United States, where rising temperatures compound increasing aridity (Udall and Overpeck 2017; Whitney et al. 2023). Streamflow declines are projected to continue (Whitney et al. 2023), increasingly threatening these native ecosystems (Scott et al. 1996; Stromberg et al. 1996; Webb et al. 2019).

Groundwater rate of recession and both inter- and intra-annual variation in alluvial groundwater levels are metrics known to affect vigour, reproduction and mortality of native riparian species, including *Salix* and *Populus* (Horton et al. 2001; Shafroth et al. 2000; Stromberg 1997). Water extraction that accelerates alluvial groundwater recession early in the growing season during *Populus/Salix* (cottonwood/willow) seed dispersal and germination can inhibit the reproductive success of these species (Rood, Braatne, et al. 2003) and depress seedling growth rate—itsself the strongest indicator of seedling survival (Stella and Battles 2010). Furthermore, native riparian seedling density has been found to be inversely related to survival and growth rate of non-native *Tamarix* (Sher et al. 2000, 2002). Thus, maintaining the hydrological processes that support successful recruitment of groundwater-dependent native riparian zones is critical for retaining them as self-sustaining ecosystems (Palmer et al. 2009).

River-floodplain lateral connectivity is a crucial determinant of hydrologic function and biological productivity in these riparian systems. Complex, branching channel forms typically exhibit higher hydrologic and sediment connectivity with their floodplains than simpler single-channel forms, more frequently inundating their floodplains and attenuating flood forces through distributary networks of floodplain channels (Cluer and Thorne 2013; Entwistle et al. 2018). These anastomosing, or branching, rivers are often found in alluvial valleys where sufficient sediment input is available (Schumm 1985) and rivers have space for dynamic processes (Skidmore and Wheaton 2022). Large floods create a complex network of ridge-and-swale features across the floodplain, which we refer to as secondary channels. Such topographically heterogeneous systems are also characterised by rich biodiversity (Kondolf 2011; Kumar et al. 2006; Polvi and Wohl 2013) and strong connections to groundwater. The patchy distribution of vegetation types across these floodplains spans the moisture spectrum from obligate wetland to xeric (Naiman and

Décamps 1997; Stromberg et al. 1996; Wohl et al. 2021). The biogeomorphological complexity and inherent feedback loops of anastomosing river systems can therefore form part of a river corridor ecosystem that is naturally resilient to the hydrologic extremes of major floods and drought (Cluer and Thorne 2013; Powers et al. 2019).

The Gila River in the Cliff-Gila Valley of southwest New Mexico is a naturally anastomosing river system that sustains a robust, expansive native riparian ecosystem while also providing water for agricultural and domestic use. Unlike in other rivers of the southwestern United States, non-native riparian vegetation (e.g., *Tamarix*; Glenn and Nagler 2005; Petrakis et al. 2023) is extremely rare in this river segment. In this work, we use 11 years of field data to examine the hydrologic and geomorphic connections that sustain this native ecosystem and may hinder encroachment by non-native species. We focused on interactions between the low flow regime and the anastomosed network of floodplain channels. Native riparian trees frequently establish along these secondary channels, suggesting that they may provide areas of improved access to groundwater for vegetation. Additionally, the breadth and complexity of the anastomosed network may help increase both the spatial extent and age-class diversity of this GDE, thereby enhancing its resilience to climate impacts like long-term drought (see Figure S1 for a conceptual diagram).

We use topographic, vegetation and continuous groundwater data for the Gila River from sites under perennial and seasonally dewatered (SD) flow conditions to address several objectives. First (Objective 1), we look at lateral connectivity between the river's perennial flows and topography across the floodplain's full width to examine the potential role of secondary channels in sustaining the riparian system far beyond the narrow corridor formed by the river's banks, even through extended periods of low flow. For Objective 2, we evaluate the possible effects of water extraction by comparing alluvial groundwater levels in the reach with seasonal flow interruption (i.e., channel dewatering) against those in perennial reaches. Finally, Objective 3 examines how maintaining small anthropogenic water inputs within the dewatered reach is related to alluvial groundwater levels and survival of native GDEs.

2 | Materials and Methods

2.1 | Site Description

The rural Cliff-Gila Valley occupies a 30-km reach of the Gila River in semiarid southwestern New Mexico, bracketed by segments of the Gila National Forest and crossing a geologic transition between the Colorado Plateau and the Basin and Range province. By the early Pleistocene, deep dissection by the Gila River and its tributaries created today's through-flowing river system (Hawley et al. 2000). Fill cycles followed, depositing coarse-grained alluvial sediments, 100–300 m deep, throughout the valleys of the upper watershed, including the Cliff-Gila Valley. The hydraulic conductivity of these materials is very high (30–90 m per day; Hawley et al. 2000; Tetra Tech Inc. 2010), which contributes to rapid alluvial groundwater movement through the river's floodplains in the Cliff-Gila Valley.

In the mid-20th century, humans profoundly simplified a complex web of main and secondary channels that had crossed the river's floodplains until at least 1935 (Figure 2; Soles 2014). By 1960, the active floodplain throughout much of the valley was confined to less than half of its historic width. Sparse native riparian forest cover and a paucity of multi-age stands reflected riparian conditions degraded by channel alignment and levee construction. These alterations probably magnified lateral shifts in the river's position throughout the valley during the following period of unusually frequent high-magnitude floods (Soles 2003; Wittler and Levish 2004), scouring fine sediments and remnant vegetation from large swaths of the floodplain. By 1980, native floodplain forest cover in the valley was reduced to 40%–50% of its early 20th century extent (Soles 2003).

Present-day conditions strongly contrast with those of the 1980s, although virtually no active restoration of the river or its riparian habitat has occurred. Channel alignment and leveeing efforts ceased by 1984, and domestic livestock were excluded from most of the valley's floodplains by the late 1990s. During the same period, frequent floods and high sediment loads typical of the Gila watershed helped return the river to its anastomosing condition. This anastomosis hydrologically connected the river's main channel surface flow with a complex network of secondary channels across the full floodplain breadth, as demonstrated in other river systems (Tockner et al. 2000). By 2000, active floodplain width was near its pre-channelization extent (300–600 m), and multiple cohorts of cottonwood, willow and other native tree species had re-colonised broad areas (Figure 2).

Like many rivers of the southwestern United States, the Gila River's streamflow derives largely from snowmelt runoff and summer monsoon rainfall (Garfin et al. 2014). Average annual precipitation ranges from 36 cm at Cliff to 45 cm in the Gila River headwaters (Western Regional Climate Center 2023). No major diversions or dams alter surface flow above the valley, but anthropogenic controls within the Cliff-Gila Valley include sediment dams on 12 tributary canyons and irrigation methods that have changed little in more than a century of use. Earthen 'push-up' berm diversions reduce summer low flows, diverting water to unlined, gravity-fed ditches that flood-irrigate fields scattered throughout the valley bottom; excess ditch flow can be shunted back to the river at several locations. These techniques create a 'leaky' system, allowing seepage below the diversion structures and from fields and ditches to eventually re-emerge as surface flow in the channel.

At the head of the valley, the river drains a watershed of approximately 3000 km², spanning elevations from 1400 to >3000 m above mean sea level (AMSL) and the river's narrow canyon broadens into a valley bottom 1200–2400 m wide (Figure 1). However, the active floodplain on which native riparian or more xeric vegetation grows is typically narrower (200–500 m), bounded by agricultural fields or berms.

Surface discharge has been continuously recorded just upstream of the Cliff-Gila Valley since 1928 (US Geological Survey [USGS] gaging station 09430500; Figure 1). The river's watershed generates a highly variable flow regime and periodically produces very large floods. The highest annual peaks since 1928 have ranged from 142 m³s⁻¹ (5000 ft³s⁻¹) to more than 991 m³s⁻¹

(35 000 ft³s⁻¹). Conversely, base flows in the river during dry periods are very low, typically 0.6–1.0 m³s⁻¹ (20–35 ft³s⁻¹). Although the river retains most of its perennial flow throughout the valley, in most years irrigation diversions dewater the stream channel downstream for periods of 2–6 weeks during low flow periods in May–September. The dewatered reach length ranges from approximately 2 km to more than 4 km in very dry years (Figure 1). During rare years with above-average discharge, perennial flow is continuous through the valley.

2.2 | Transect Topography and Vegetation Mapping and Analysis

To address Objectives 1 and 2, we established 13 study transects in 2007–2009 that characterise floodplain topography and vegetation and their relationship with the river's surface flow regime and groundwater (Table S1 and Figure S2). The transects were oriented perpendicular to the river and irregularly spaced throughout the Cliff-Gila Valley, subject to accessibility. Surface flow was perennial at 11 sites, perennial most years at one site and seasonally dewatered every year at one site. Transects with perennial flow were positioned to bracket the SD segment. To evaluate groundwater response relative to both variations in surface flow and distance from the main channel, we installed and instrumented three to four shallow groundwater monitoring wells on eight of the 13 transects. Groundwater data were recorded over time periods ranging from four to 14 years. For this study, we focus on three transects with continuous data over the longest overlapping period of groundwater data availability (2011–2021).

The selected transects allowed examination of a range of hydrologic conditions and associated habitats (Figures 1 and S3). The upstream perennial (UP) transect is located upstream of all irrigation diversions, approximately 4 km downstream of the USGS gaging station. The SD transect, about 2 km downstream of the UP transect, is positioned approximately halfway through the river segment that is seasonally dewatered during most years. Perennial surface flow is restored farther downstream, where discharge was usually at least 95% of discharge at the USGS gaging station (Propst 2019). The downstream perennial (DP) transect is located downstream of all irrigation diversions and restored perennial flow, a short distance below the Highway 180 bridge over the river. The total study reach length is approximately 20 river km (Figure 1).

To monitor the evolving floodplain and channel, we used a total station (Topcon GTS-226) to map detailed topography across each transect in 2013, 2014 and 2018, spanning the valley bottom for a width of 400–600 m. Surveys document conditions bracketing high-magnitude floods that occurred during the study period in September 2013 and December 2016 and were conducted in late fall or winter when vegetation was dormant ('leaf-off') to aid visibility. At each transect, multiple permanent controls (i.e., 3/4-in. iron rods or 5/8-in. rebar) were established to provide measurement repeatability over time. Internal survey accuracy was ±2 cm vertical and ±3 cm horizontal. Final transformation of the survey grid and datum coordinates used points collected by high-accuracy GPS at two to three controls on each transect (±0.2 m vertical accuracy).

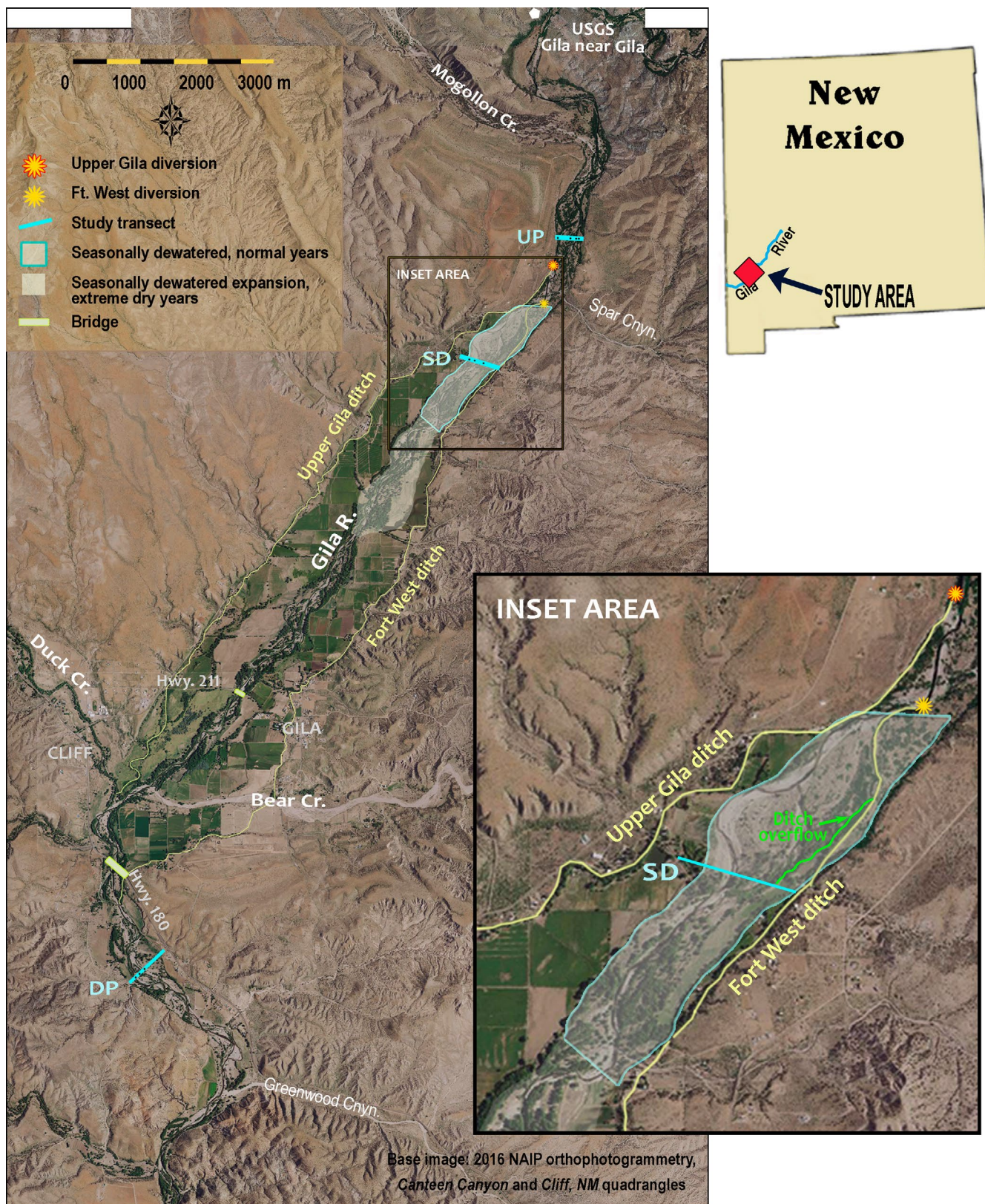


FIGURE 1 | Study reach in the Cliff-Gila Valley, showing the three study transect locations for this work: upstream perennial (UP), seasonally dewatered (SD) and downstream perennial (DP); major irrigation diversion sites and the approximate regions where the channel was seasonally dewatered by diversions in normal and extremely dry years. The dewatered region is magnified in the inset figure to show the position of the Fort West ditch overflow channel. USGS gaging station 09430500 is located at the upstream end of the valley. Gila River flows from north to south.

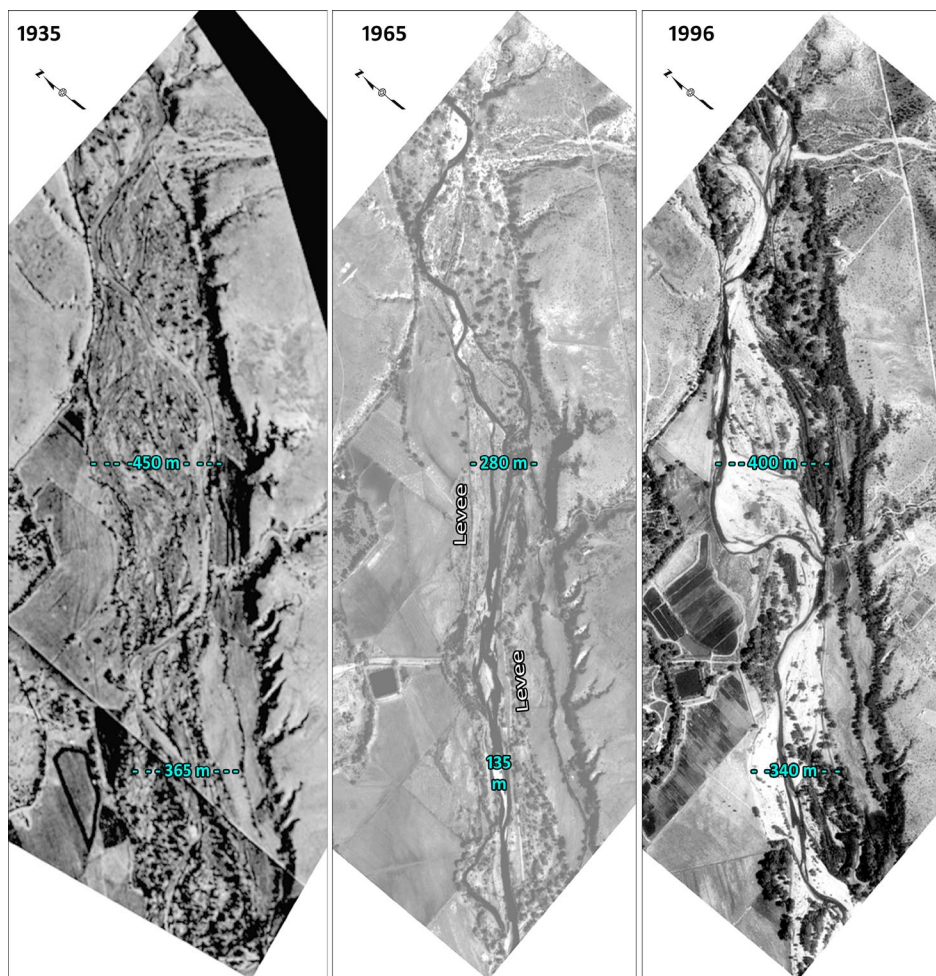


FIGURE 2 | Aerial photos from 1935, 1965 and 1996 of the upstream Cliff-Gila Valley show the reduction in active floodplain extent imposed by levee construction between 1940 and 1965 and re-widening of the floodplain by frequent high-magnitude floods, 1978–1996. Flood scour and channel avulsion left a network of secondary channels across floodplains by 1996 similar to those present in 1935. 1935 imagery from US National Archive, scale unknown. 1965 imagery from US Bureau of Land management, scale 1:18000. 1996 imagery from US Geological Survey, scale 1:24000.

During each survey, we also mapped 11 classes of vegetation (Table 1) crossing each transect. We focused on these classes to enable an efficient and repeatable method for mapping floodplain vegetation in relation to floodplain topography. Because similar vegetation classes or communities (e.g., cottonwood/willow stands, upland shrubs) typically occupy areas oriented roughly longitudinal to the main channel, these appear as ‘bands’ of varying width crossing the transect (Figure 3). The width of each vegetation class crossing the transect was mapped, enabling evaluation of relationships among vegetation classes and alluvial groundwater depths across years. Bands were mapped contiguously (i.e., the end of one band always marked the start of the next). Bands of mature (gallery) cottonwood were distinguished from younger trees and seedlings because of this species’ specific hydrologic requirements for germination and early survival (seedling through sapling stage; Rood, Braatne, et al. 2003). Only one vegetation class was assigned per band and as the dominant floodplain forest type, where cottonwood/willow canopy was present, other vegetation types were subsumed. The total widths of all bands of each vegetation class were summed and divided by the total transect width to calculate the percent cover of each class (e.g., of young cottonwood/willow). To determine whether vegetation bands on the three

study transects were representative of floodplain vegetation valley-wide, we compared them with data mapped on the 13 original transects (see Section S2 in Supporting Information).

2.3 | Groundwater and Surface Water Hydrology

For Objectives 1 and 2, we also recorded alluvial groundwater levels for water years (WYs; as used here, WY begins October 1 and ends September 30 of the following year and is designated by the calendar year in which it ends) 2011–2021 with pressure transducers (Solinst Corp). Groundwater data were recorded in several wells on each of the study transects (Table 2) at a 30-min time step to capture the abrupt and transient increases in floodplain groundwater level that accompany Gila River flow pulses. Effects of barometric pressure on groundwater level were adjusted in Levellogger software (v. 4.2, Solinst 2012) using simultaneous barometric data recorded by a Barologger (Solinst Corp.) placed within 5 km (3 miles) of each well. For each well and each year, we calculated seasonal maximum, minimum and median groundwater levels, as well as 90th and 10th percentiles, in Microsoft Excel 2019. We derived hydrologic seasons for our analyses by modifying Horner and Dahm’s (2014) classification

TABLE 1 | Floodplain vegetation classes mapped during transect surveys with examples of indicator species.

Habitat class	Indicator species examples
None (barren)	None
Obligate wetland/wet meadow	Obligate or facultative herbaceous (e.g., sedge; rush)
Grass/forb (upland)	Native and/or non-native grass, forb (e.g., <i>Grama</i> spp.; <i>Bassia scoparia</i>)
Riparian (mesic) shrub	Seepwillow (<i>Baccharis salicifolia</i>); New Mexico olive (<i>Forestiera neomexicana</i>)
Upland (xeric) shrub	Rabbitbrush (<i>Ericameria</i> spp.); snakeweed (<i>Gutierrezia sarothrae</i>)
Riparian (mesic) forest: cottonwood/willow, young	<i>Populus/Salix</i> (seedling, sapling)
Riparian (mesic) forest: cottonwood/willow, mature	<i>Populus/Salix</i> (mature gallery)
Riparian (mesic) forest: native mixed broadleaf	Box elder (<i>Acer negundo</i>); alder (<i>Alnus oblongifolia</i>); sycamore (<i>Platanus wrightii</i>)
Transition/upland forest (native)	Hackberry (<i>Celtis reticulata</i>); desert willow (<i>Chilopsis linearis</i>); walnut (<i>Juglans major</i>); Juniper (<i>Juniperus</i> spp.); mesquite (<i>Prosopis</i> spp.)
Non-native forest	Siberian elm (<i>Ulmus pumila</i>); tamarisk (<i>Tamarix</i> spp.); tree of heaven (<i>Ailanthus altissima</i>)
Cultivated (historical or present)	

Note: *Populus/Salix* (cottonwood/willow) stands were mapped as either young (pole/sapling) or mature (gallery).

of ecologically significant patterns of discharge within the Gila watershed into four periods: November–January (winter base flows); February–April (snowmelt runoff); May–July (lowest flows) and August–October (monsoon).

Instantaneous streamflow data for WY 2011–2021 were obtained from USGS gaging stations 09430500 (Gila near Gila) and 09430600 (Mogollon Creek), both located upstream of the UP transect and all Cliff-Gila Valley diversions (United States Geological Survey 2022a, 2022b). Daily diversion data for the Upper Gila and Fort West irrigation ditches were obtained from New Mexico Office of the State Engineer for WY 2011–2021 (Office of the State Engineer 2022). These ditches divert streamflow near the upper end of the valley. We subtracted ditch flows

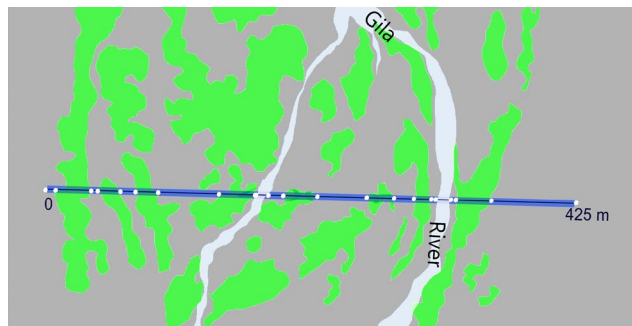


FIGURE 3 | Simplified schematic of a typical study transect (425-m long black line) and the 10-m transect belt (blue shading) for aerial photography analysis. Green polygons represent single contiguous 'bands' of similar vegetation and white dots mark points surveyed at each edge of a vegetation band to map the band's width where it crossed the transect. In the air photo analysis, we digitised the area within each vegetation polygon where it overlapped the 10-m belt.

from total Gila and Mogollon discharge to calculate surface flow for periodically dewatered conditions (see Section S1 in Supporting Information).

2.4 | Relationship of Seasonal Dewatering to Alluvial Groundwater

To evaluate differences in rates of groundwater recession and depths to water (DTW) under seasonal dewatering versus perennial flow conditions (Objective 2), we identified the onset date of dewatering at the SD transect each year from the streamflow and ditch gages data and compared the relative changes in alluvial groundwater levels among the three transects during the initial dewatering period. We selected data from one well on each transect for the comparison (Table 2) and conducted Kruskal–Wallis one-way analysis of variance (ANOVA) on ranks in SigmaPlot v. 14.5; pairwise comparisons by Tukey's HSD post hoc test quantified the differences between groups.

The SD transect was situated downstream of irrigation diversions where surface flow is depleted and the channel periodically dewatered. Anthropogenic water inputs near both ends of the transect can raise water levels in all three wells on the transect, but their influence is minimised in the centre well (WCtr) nearest the active channel. Therefore, data from this center well, positioned on the relatively flat west floodplain, best represented seasonal dewatering effects and were selected for comparison with data from one well on each perennial transect (i.e., UP and DP) to address Objective 2.

Wells selected for comparison on the perennial transects were situated at similar distances from the active channel and similar elevations above the channel thalweg as WCtr on the SD transect (Table 2). On transect UP, well UP WCtr was originally positioned on the right bank of a secondary channel about 75 m off the active channel in 2011. High-magnitude flooding in late 2016 shifted most surface flow to an abandoned channel farther west on the transect, about 165 m from UP WCtr. Well DP E2 was positioned about 105 m from the active channel, adjacent to a broad secondary channel on the left floodplain.

TABLE 2 | Details about observation wells used in this study.

Transect well ^a	Average distance to channel edge (m) ^b	Geomorphic surface	Ground elevation above thalweg (m)
UP E	20/255	Terrace	3.7
UP Ectr	6/243	Channel edge	1.6
UP WCtr	75/165	Floodplain	2.4
UP W	245/7	Floodplain	1.3
SD E	60	Floodplain	2.7
SD WCtr	90	Floodplain	2.5
SD W	145	Floodplain	3.1
DP E1	180	Floodplain	1.8
DP E2^c	105	Floodplain	2.2
DP E3	12	Channel edge	1.4

Note: Data from wells in bold were used for calculations of depths to water (DTW) and groundwater recession rates under the different flow conditions shown. UP designates wells in the upstream perennial reach; SD designates wells in the seasonally dewatered reach; and DP designates wells in the downstream perennial reach. ^aWells are listed in east-to-west order for each transect: E = east of river; W = west of river; Ctr = nearer to river.

^bFor UP wells, the distances shown are prior to/after 23 December 2016, when high-magnitude flooding and upstream aggradation re-avulsed the channel to its historical position on the west floodplain margin.

^cOn the DP transect, only well E2 was present 2011–2013. A groundwater slope of 0.002 calculated from low flow periods after 2014 was used to estimate DTW across the transect in 2011–2013.

2.5 | Alluvial Groundwater–Topography Relationships

We used data from all wells on each of the study transects (Table 2) in combination with detailed topography mapped along the transect to calculate DTW across each transect (Leenhouts et al. 2006), with special emphasis on groundwater depths beneath vegetated secondary channels crossing each transect. We identified secondary channels from survey data and included in the analyses only those occupied by a vegetation type that also occurred at both other transects; for example, channels occupied by ‘other native riparian trees’ (sycamore, box elder) were excluded because they occur only at the UP transect. In addition, we included only secondary channels at least 5 m in width to avoid overstating the effects of multiple very narrow channels within a short distance (e.g., two channels occupying a span of 8 m were considered a single channel). See Section S3 in Supporting Information for detailed methods for calculating DTW below secondary channels. To address Objective 1 and especially the focus on water stress (i.e., drought) effects on vegetation, we evaluated relationships among these channels, DTW and vegetation type during the months of greatest water scarcity, May–July. We calculated 90th percentile DTW (i.e., the deepest 10% of all DTW as the dependent variable that would indicate high water stress) beneath all secondary channels crossing each study transect during May–July of each year. We analysed pairwise differences among 90th percentile DTW by transect and by vegetation class (independent variables) via Kruskal–Wallis ANOVA on ranks in SigmaPlot (v. 14.5). Post hoc pairwise multiple comparisons used Dunn’s method because the number of secondary channels varied among transects.

To address Objective 3, data from the SD transect were additionally evaluated for effects of small water inputs by overflows shunted from the Fort West ditch (Figure 1, inset) by separately

analysing results for secondary channels near (i.e., within 100 m) and distant from this water source. Secondary channels most distant from the overflow were those nearest (i.e., within approximately 100 m) to the river channel and vice-versa. We calculated these 90th percentile DTW values for the May–July period and compared them with 90th percentile DTW values from the UP and DP transects, again using Kruskal–Wallis ANOVA on ranks as described above, with the 90th percentile DTW values as the dependent variable and the study transects as independent variables.

3 | Results

3.1 | Alluvial Groundwater, Secondary Channels and Vegetation Interactions

3.1.1 | Flow Regime Variability

The extraordinary variability of the Gila River’s natural hydrograph is well-documented (Horner and Dahm 2014; United States Geological Survey 2022a, 2022b). Rapid changes in river stage caused by brief flow pulses are mirrored in alluvial groundwater data (Figure 4a–d). During the 11-year study period, two high-magnitude floods exceeded the 10-year recurrence interval (RI) described in Horner and Dahm (2014) (Figure S4). In September 2013, discharge rose from 8.5 to 425 m³ s⁻¹ (300–15000 ft³ s⁻¹) in 8 h and peaked 3 days later at nearly 850 m³ s⁻¹ (30000 ft³ s⁻¹), nearing the 50-year RI. In December 2016, discharge rose sharply from 14 m³ s⁻¹ (500 ft³ s⁻¹) to more than 455 m³ s⁻¹ (16000 ft³ s⁻¹) in less than 15 h. Both events resulted in lateral movement at and near the main channel on all three transects (Figure 5a–c); the smaller flood in December 2016 shifted the main channel on the UP transect more than 150 m to the west. Although both floods deposited substantial sediment and large piles of flood debris across

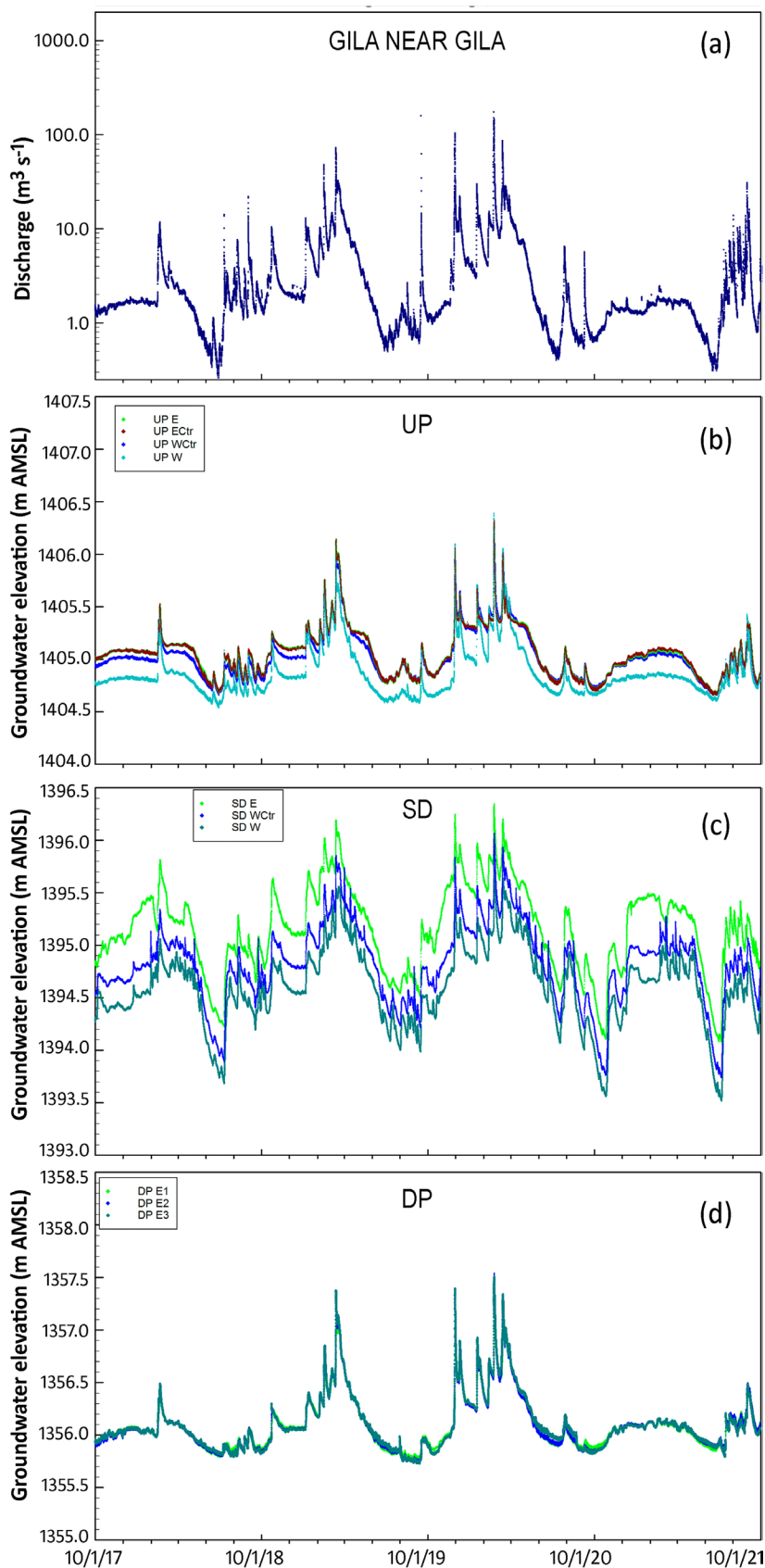


FIGURE 4 | Representative surface flow and alluvial groundwater levels in the Cliff-Gila Valley during part of the study period, WYs 2018–2021 (for clarity, other years are omitted). Data are reported at a 30-min time step for (a) Total surface flow at the upstream perennial (UP) transect, as recorded at USGS 09430500 (Gila near Gila) and USGS 09430600 (Mogollon Creek) gages; (b) Groundwater levels in wells on UP transect; (c) Groundwater levels in wells on seasonally diverted (SD) transect and (d) Groundwater levels in wells on downstream perennial (DP) transect. Well locations are in Table 2.

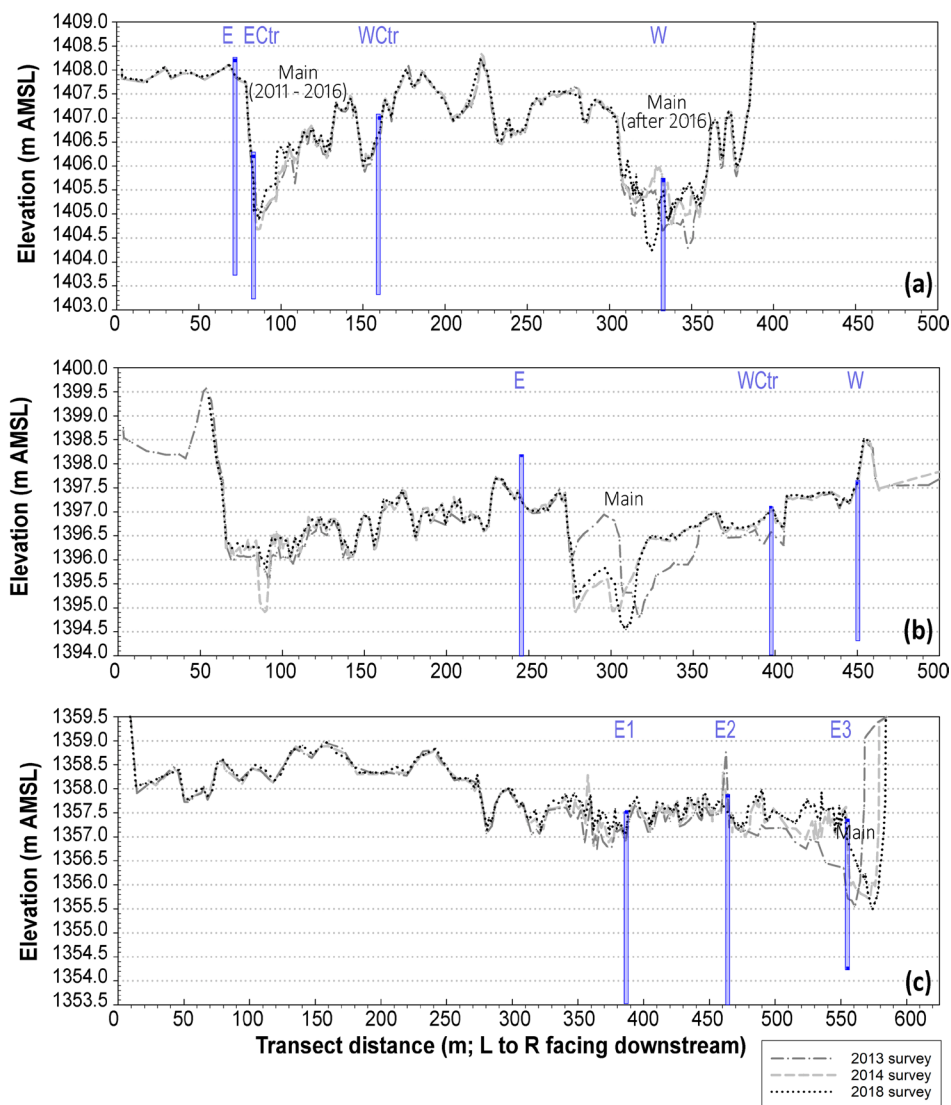


FIGURE 5 | Elevations of the three study transects as surveyed in 2013, 2014 and 2018 at (a) upstream perennial (UP) transect; (b) seasonally de-watered (SD) transect; and (c) downstream perennial (DP) transect. Vertical blue lines mark well positions on each transect; wells are labelled across the top of each graph. Each vertical axis spans 6m. 'Main' indicates position of main channel.

floodplains (M. Cooper, personal obs.), lateral movement among secondary channels was minimal (Figure 5a–c).

At the other extreme, surface flow in perennial reaches often declined below $0.85\text{ m}^3\text{ s}^{-1}$ ($30\text{ ft}^3\text{ s}^{-1}$; Figure S4) during the driest months (May–July; Horner and Dahm 2014). In 6 of 11 years between 2011 and 2021, daily mean low flows at the Gila gaging station 09430500 were $<0.6\text{ m}^3\text{ s}^{-1}$ ($20\text{ ft}^3\text{ s}^{-1}$) for periods of up to 4 weeks. Through WY 2021, however, recorded daily mean discharge at the gaging station was never less than $0.3\text{ m}^3\text{ s}^{-1}$ ($10\text{ ft}^3\text{ s}^{-1}$).

3.1.2 | Vegetation Distribution

Comparisons of riparian vegetation cover datasets in 2011, 2013 and 2018 indicated that our vegetation mapping methods produced results for the three transects that were roughly representative of floodplain vegetation valley-wide, with total percent cover of all mesic and riparian vegetation varying by less than

1.1% among the three datasets (Figure S5). Native riparian trees and mesic shrub species occupied nearly 33% of mapped transect widths, especially cottonwood (*Populus fremontii*, *Populus angustifolia* and hybrids) and willow (e.g., *Salix gooddingii* and *Salix exigua*). Other species included Arizona sycamore (*Platanus wrightii*), box elder (*Acer negundo*), Arizona walnut (*Juglans major*), velvet ash (*Fraxinus velutina*), seepwillow (*Baccharis salicifolia*) and Arizona alder (*Alnus oblongifolia*). As noted earlier, non-native trees are sparse in the Cliff-Gila Valley, occupying $<0.2\%$ of the floodplain in each of the 3 years.

Analysis of vegetation distributions relative to main channel proximity showed that the large majority of native riparian trees and shrubs grew in floodplain zones more than 20m distant from the active channel (Figure 6a–c). In other words, most wetland and mesic vegetation species associated with the Gila River are not restricted to zones near the main channel but are patchily distributed across the entire floodplain. Analysis of vegetation distributions across transects also showed that riparian species, especially young cottonwood/willow, were most

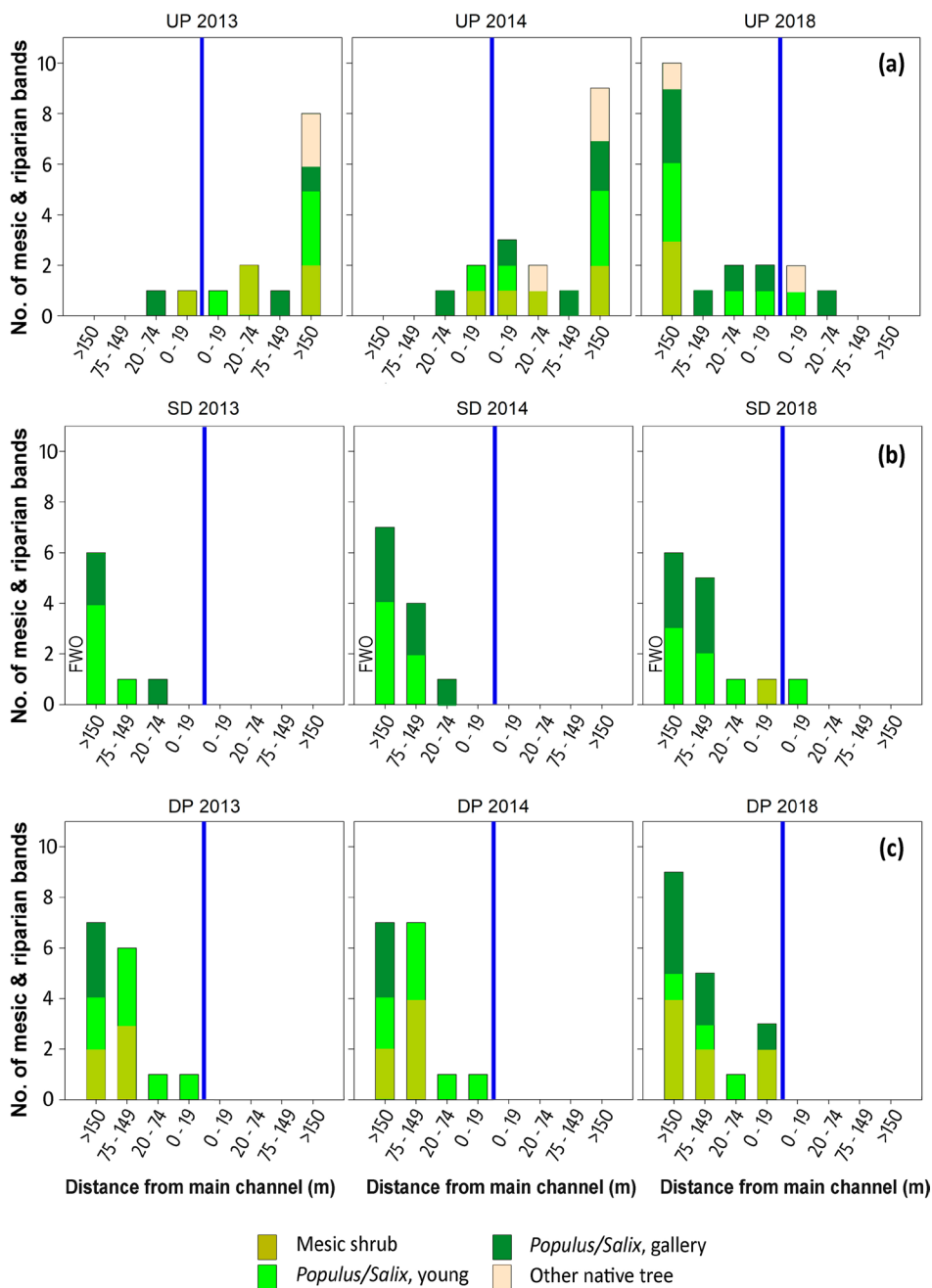


FIGURE 6 | Distribution of riparian and mesic vegetation across floodplains during surveys in 2013, 2014 and 2018 on transects (a) upstream perennial (UP); (b) seasonally dewatered (SD) and (c) downstream perennial (DP). The blue vertical line marks the main channel position; stacked bars represent the number of riparian bands crossing the transect, within the x axis distances shown, on the floodplains to the left (east) and right (west) of the channel. The Fort West ditch overflow channel (‘FWO’) provides small amounts of additional water on the SD transect approximately 200m left of the main channel.

frequently associated with secondary channels at the UP and SD transects, but less often at the DP transect.

Changes in vegetation cover followed each high magnitude flood event (in 2013 and 2016) and some areas of floodplain topography were substantially reworked (Figure 5). For example, we observed successful recruitment and growth of native riparian species at all three sites after the large 2013 flood (Figure 6). At the UP transect between 2013 and 2014, new bands of riparian vegetation were established adjacent to the main channel and > 150m distant from it. New growth was also present in 2014 at

transect SD near the Fort West overflow between 75 and > 150m from the main channel. At transect DP, at least one new band of riparian vegetation was established 75–150m from the main channel edge between 2013 and 2014.

Riparian vegetation, mostly > 150m distant from the active channel, occupied both floodplains at the UP transect (Figure 6a) during all surveys. There was no change in the total number of riparian bands on the transect between 2016 and 2018, although channel avulsion during the large flood in late 2016 shifted the main channel far west of its previous position, broadening the

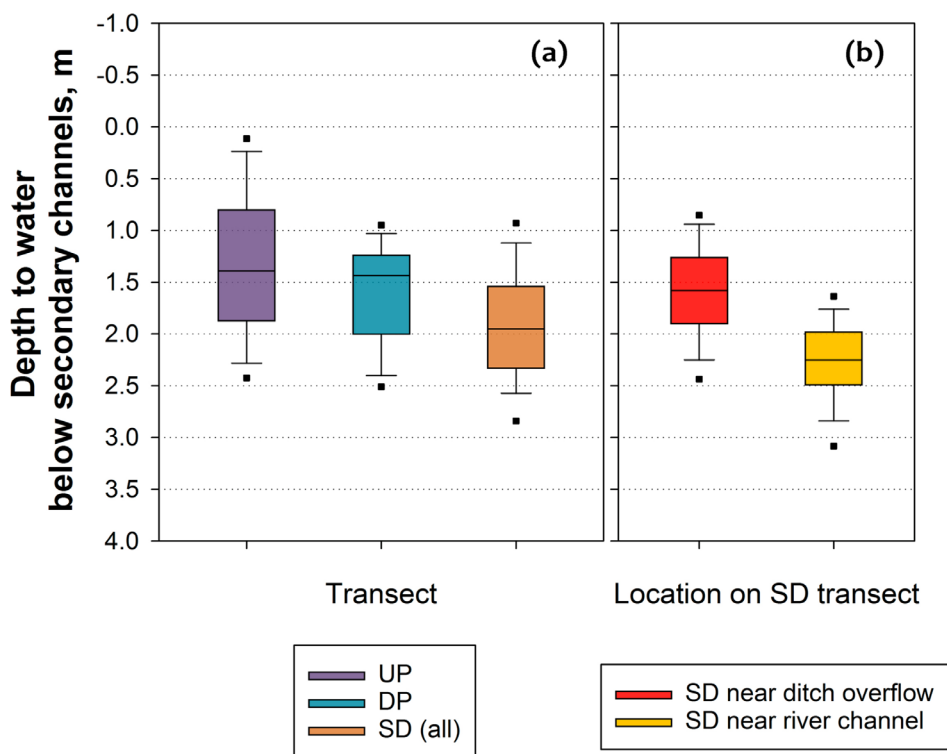


FIGURE 7 | Box plots of 90th percentile depths to water below secondary channels during the study period: (a) May–July, at perennial transects UP and DP, and the seasonally dewatered (SD) transect; (b) May–July, at secondary channels nearest the Fort West ditch overflow on the SD transect (left) and farthest from the ditch overflow (i.e., nearest the river channel). For each box plot, data are plotted relative to the ground surface at each transect, with negative values indicating above-ground water levels. Each box outlines the 25th–75th percentile values within each data set, with the horizontal line indicating median values; whiskers and outlier boxes indicate 10th/90th and 5th/95th percentile values, respectively.

east floodplain. Consequently, more riparian bands occupied the east floodplain after 2016.

At both the SD and DP transects (Figure 6b–c), riparian vegetation in nearly all years was restricted to the east floodplain. On the SD transect, no riparian recruitment occurred distant from the main channel between 2014 and 2018, but thin bands of vegetation were established on the main channel margins. On the DP transect, all riparian recruitment was restricted to the east bank where, by 2018, two new vegetation bands were established and riparian cover increased substantially.

3.1.3 | Secondary Channels and DTW

To evaluate Objective 1, we identified all vegetated secondary channels that crossed each study transect (14–20 per transect survey). For each channel, we calculated annual 90th percentile depth to water (DTW) during the period of highest water stress (May–July, per Horner and Dahm 2014) beneath the lowest point (thalweg). Secondary channels were typically far from the main channel, at an average distance of 190 m. The 90th percentile DTWs below secondary channels at the DP transect varied least, remaining within a range of about 1.4 m; most (80%) of the 90th percentile DTWs on the UP and SD transects varied more, within ranges of about 2.0 and 1.6 m, respectively (Figure 7a). Statistical analysis of annual extreme values (i.e., 90th percentiles) calculated from the secondary channel DTWs for May–July indicated that the difference between 90th percentile values among all three transects was statistically significant, with

$p < 0.001$ between the SD and UP (N (SD)=179; N (UP)=168) and between the SD and DP transects (N (DP)=214), while the least significant difference in DTWs was between the UP and DP transects ($p = 0.033$).

We also compared 90% percentile DTWs (dependent variable) in May–July among secondary channels occupied by three vegetation types (independent variables) across all three transects: gallery and young cottonwood/willow and grass/forb. Statistically significant differences were found among all three vegetation types ($p < 0.001$; $N = 33$). DTW was greatest in grass/forb bands (average 90th percentile DTW = 2.5 m), followed by mature cottonwood/willow (2.0 m). DTW was least (1.5 m) for young cottonwood/willow. In other words, young-cottonwood/willow established itself nearest to groundwater in the deepest secondary channels.

3.2 | Seasonal Dewatering Relationships to Groundwater Recession

During the study period, two upstream points of diversion (for the Upper Gila and Fort West ditches) reduced streamflow by an average total of about $1.13 \text{ m}^3 \text{ s}^{-1}$ ($40 \text{ ft}^3 \text{ s}^{-1}$) near the head of the Cliff-Gila Valley (Figure S4). In most years, as the natural hydrograph dipped to $1.13\text{--}1.42 \text{ m}^3 \text{ s}^{-1}$ ($40\text{--}50 \text{ ft}^3 \text{ s}^{-1}$) by late spring, the diversions captured all available streamflow, dewatering a segment of the river channel (Figure 1). Perennial flow re-emerged upstream of the Highway 211 bridge near Gila when fed by sufficient hyporheic flow, tailwater returns and seepage from ditches and fields.

TABLE 3 | Onset dates of earliest extended channel dewatering at site SD and length of initial dewatered period, water year 2011 through 2021.

Onset of channel dewatering		Length of initial dewatering period (days)
Water year	Date	
2011	June 4	33
2012	May 21	36
2013	May 22	34
2014	June 12	23
2015	June 7	18
2016	June 7	40
2017	June 26	20
2018	May 22	26
2019	May 15	37
2020	June 25	24
2021	June 8	16

Note: Onset of channel dewatering refers to locations below the Fort West diversion (see Figure 1).

Temporal and spatial extents of dewatering depend on antecedent conditions, local climate factors and duration of low flow conditions. From 2011 to 2021, extended periods of dewatering were most often initiated in late May to early June (Table 3) and lasted for 2 to nearly 6 weeks. Extended dewatering began as early as May 15; it was delayed into late June in 2 years (2017 and 2020). Sporadic monsoon flow pulses usually generated occasional surface flow through the reach following initial dewatering, especially beginning in late July, but intermittent dewatering often continued into September or October.

To address Objective 2, we plotted relative annual groundwater level declines at the selected wells on the three transects (Table 2) during extended periods of steep recession at well SD Wctr (Figure 8a–c) that persisted over periods ranging from 16 days (in 2021) to 40 days (in 2016). The median period of steepest decline was 26 days. Diversion and dewatering greatly increased the rate of alluvial groundwater level decline at SD Wctr (Figure 8b) relative to the perennial site wells, UP Wctr (Figure 8a) and DP E2 (Figure 8c). At the perennial reaches, alluvial groundwater levels fell at a median daily rate of 0.3 cm day⁻¹ (at UP) and 0.1 cm day⁻¹ (at DP) over these periods. The median rate at SD Wctr was 2.2 cm day⁻¹ over the same periods and year-to-year variation was much greater than at the perennial sites. Rates of recession at SD Wctr ranged from slightly less than two times that at perennial sites (in 2019) to 25 times the rate at perennial sites (in 2020). Results of the Tukey test comparing log-transformed median rates of recession for each year showed statistically significant differences between the UP and SD wells and between the DP and SD wells ($p < 0.001$ and $p = 0.005$, respectively), but no statistically significant difference existed between median rates of recession for the UP and DP transects ($p = 0.182$).

Average daily groundwater recession rates at each well site were compared to seedling mortality ranges for native phreatophytes documented in previous studies (Figure 9). Mahoney and Rood (1998) identified a decline of about 2–4 cm day⁻¹ as the maximum survivable by first-year cottonwood seedlings. Stella et al. (2010) documented > 50% mortality among cottonwood and willow seedlings after 35–46 days of 3 cm day⁻¹ drawdown in experimental studies. At SD Wctr, the median rate of recession during periods of extended groundwater decline exceeded 2 cm day⁻¹ in 7 of 11 years and neared or exceeded 3 cm day⁻¹ in 2 years, but at the perennial sites, median groundwater levels receded at < 1 cm day⁻¹ in all years. Furthermore, maximum rates of groundwater recession (not shown) at the SD well reached 2–4 cm day⁻¹ in all years for at least a few days.

3.3 | Effects of Supplemental Water Inputs

Groundwater levels across the full extent of the SD transect reflect not only channel dewatering effects, but also sporadic inflow of excess water shunted off the Fort West ditch (Figure 1 inset). Well SD E is nearest to supplemental ditch inputs and groundwater levels there were uniformly the highest on the transect (Figure 4c). Although discharge in the ditch overflow channel was not quantified, multiple site visits during May–July documented that any flow present typically reaches the east end of the transect as a steady trickle so long as flow diverted into the Fort West ditch is above ditch capacity.

For Objective 3, we compared groundwater levels near the supplemental ditch inputs and those nearer the main channel. The 90th percentile (high water stress) DTW beneath secondary channels near the ditch overflow were similar to those at the perennial transects (Figure 7b). At the other end of the transect, near the main channel, seasonal dewatering effects on groundwater levels were more evident. There, 90th percentile DTW below secondary channels during May–July ranged from about 1.7–2.7 m.

Analysis of 90th percentile May–July DTW beneath secondary channels at all four sites (UP, DP and the two SD sites) by Kruskal–Wallis ANOVA on ranks and Dunn's multiple pairwise comparisons identified statistically significant differences between the right (dewatered) end of the SD transect ($N(\text{SDR}) = 88$) and all other sites ($N(\text{UP}) = 168$; $N(\text{DP}) = 214$; $N(\text{SDL}) = 91$; $p < 0.001$). No statistically significant difference existed between the perennial UP transect and the water-supplemented left end of the SD transect ($p = 0.157$; $N(\text{UP}) = 168$; $N(\text{SDL}) = 91$). In other words, the ditch overflow generated groundwater levels that were similar to those at the UP flow site.

4 | Discussion

The work presented here used a long-term dataset to examine relationships between groundwater, topography and the vegetation community of the riparian GDEs of the Gila River, a naturally anastomosing river that retains a relatively natural flow regime. In particular, we considered the role of secondary channels in contributing to riparian vegetation distribution, how

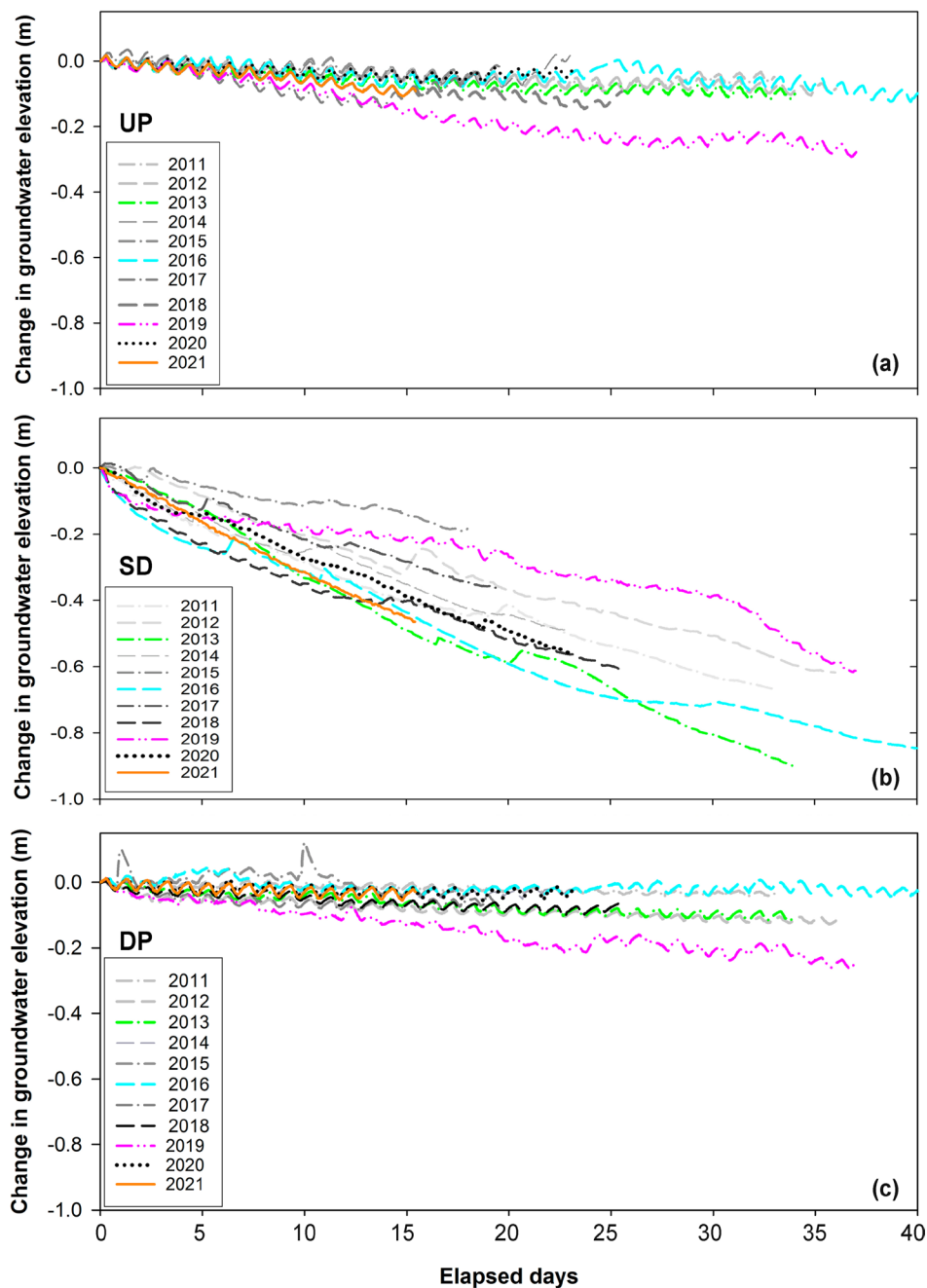


FIGURE 8 | Change in alluvial groundwater levels over time each year at wells on transect (a) UP; (b) SD and (c) DP, during initial periods of channel dewatering and extended groundwater decline at SD, 2011–2021. For each well, initial groundwater level is set to zero, and the y axis spans 1 m. Table 3 lists onset dates. The DP reach is downstream of ephemeral tributaries Duck and Bear Creek, which can contribute brief, rare surface flow in the early growing season. Groundwater pulses in 2017 at this site, for instance, were probably caused by brief surface flow from one or both tributaries.

diversions and seasonal dewatering affect groundwater levels and the value of supplementing small amounts of water to support the riparian ecosystem.

4.1 | Importance of Secondary Channels to Hydrologic Connectivity and Vegetation Distribution (Objective 1)

Anastomosis on the Gila River in the Cliff-Gila Valley after 1980 created an extensive network of secondary channels

across the river's broad floodplains. As in similar river systems, secondary channels on the Gila River's floodplains often roughly parallel the active river channel, branch into other channels and eventually rejoin the main channel, creating enormously complex floodplain topography (Henriques et al. 2022), a crucial structural component of connectivity in the Cliff-Gila Valley. This work demonstrated that at perennial sites, even secondary channels distant from the main river channel improve groundwater accessibility for native groundwater-dependent riparian trees, expanding the spatial extent of sites suitable for their potential recruitment and

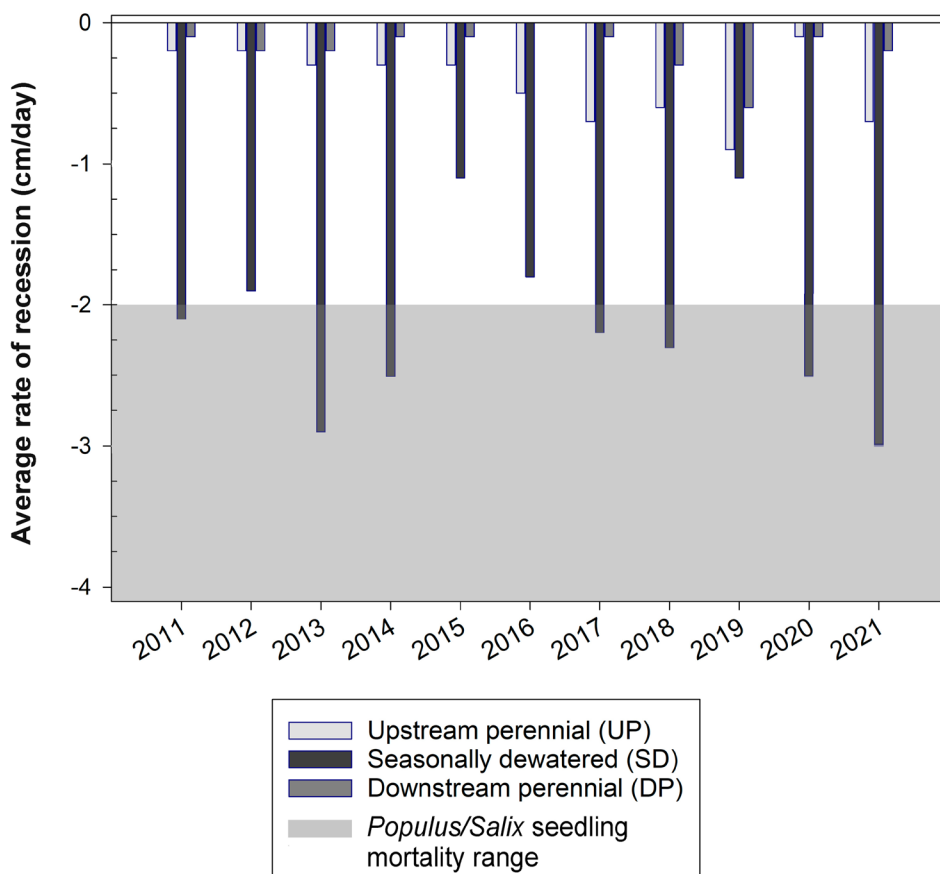


FIGURE 9 | Median daily rates of groundwater recession each year during extended periods of groundwater recession (Table 3) at perennial transects UP and DP, and at seasonally diverted transect SD. Grey shading indicates the approximate reported mortality threshold range for native tree seedlings (e.g., *Salix* (willow); *Populus* (cottonwood)).

survival. Normally dry secondary channels are not only inundated during floods (e.g., by flows during elevated spring runoff, often considered fundamental to successful recruitment of native mesic vegetation), but in many years become hydrologically connected to rising river stage as alluvial groundwater levels increase enough to moisten the channel beds (Figure S1). Thus, secondary channels can provide conditions essential to germination of the wind-dispersed seeds of *Salicaceae* even when carrying no surface flow. At perennial sites, successful recruitment of cottonwood, willow or baccharis is additionally favoured by slow groundwater recession rates ($< 1 \text{ cm day}^{-1}$; Figure 9), sustaining young bands of native riparian trees far from the main channel (Figure 6a,c). Other work has described secondary channels as prime riparian recruitment zones, providing multiple advantages for native seedling establishment (Rood, Braatne, et al. 2003), including enhanced connectivity with alluvial groundwater, offering moist zones favourable to native seedling survival (Henriques et al. 2022; Shafroth et al. 2000) and fostering expansion of diverse, multi-generational native riparian species across the full extent of the river's broad floodplain.

Very low alluvial groundwater levels can occur in August–October, but these extremes are typically short-lived, punctuated by monsoon flood pulses; groundwater levels are lowest in May–July. Even through May–July, we found that the majority of 90th percentile (high water stress) DTWs at

perennial sites remained within 2.0 m below secondary channels (Figure 7a), providing important water accessibility for young riparian trees (Lite and Stromberg 2005; Stromberg et al. 1996). The deepest segments of secondary channels can remain wet year-round and are colonised by obligate wetland species like *Typha* or *Juncus* (Soles, personal obs.), adding to the ecosystem's diversity.

Where secondary channels were absent, as on the west side of the DP transect, mesic vegetation recruitment was minimal or non-existent and generally constrained to surfaces adjacent to the main channel (Figure 6b–c), where seedlings may be lost during large flood events. For example, in 2022, large floods subsequent to our study period scoured away young trees at the SD transect that had taken root near the main channel before 2018 (Figure 6b), but young vegetation established along secondary channels that were inundated during this event generally survived (Soles, personal obs.). Vegetation along these secondary channels also dissipates the hydraulic force of large floods, creating sites of sediment capture during these events (Entwistle et al. 2018; Henriques et al. 2022). Such processes over multiple floods can leave substantial deposition (Figure 5; Rood, Gourley, et al. 2003), eventually burying tree root collars by $> 1 \text{ m}$. This effect was confirmed by our results showing that average high water stress DTWs in secondary channels occupied by older cottonwood/willow bands were greater (by approximately 0.5 m) than among younger trees of these species.

4.2 | Diversions and Seasonal Dewatering Relationship to GDE Resilience (Objective 2)

Interactions between anthropogenic and GDE needs were particularly evident in the SD reach, where hydrologic connectivity was reduced by agricultural diversions. Groundwater recession at well SD WCtr abruptly increased when the channel was dewatered, in some years nearing reported mortality thresholds for native riparian seedlings (Figure 9) during periods crucial to native riparian forest recruitment (Table 3). Limited recruitment was observed on the west side of the SD transect where dewatering was most pronounced (Figure 6b), suggesting that groundwater recession during extended drought periods expected under a changing climate may exceed rates for longer periods of time that are lethal to seedlings. Flow disruption later in the growing season can reduce or eliminate initially successful cottonwood/willow recruitment because first-year seedlings and young saplings are particularly susceptible to groundwater scarcity (Lite and Stromberg 2005; Lytle and Merritt 2004; Smith et al. 1998). Juvenile cottonwood roots can grow 60–100 cm in their first year (Braatne et al. 1995; Mahoney and Rood 1998) and groundwater depths near the main channel in the SD reach often approached or exceeded these limits during the study period (unpublished data). In fact, much of the existing gallery cottonwood/willow in this reach was established during the late 1990s, when relatively high median monthly streamflow in May and June was sufficient to generate perennial flow through the SD reach in these months, sustaining groundwater levels.

4.3 | Importance of Supplemental Water Inputs (Objective 3)

Alluvial groundwater is an essential component for reproductive success, vigour and survival of native wetland and riparian GDE species, strongly influencing the composition and resilience of floodplain vegetation (Gonzalez et al. 2018; Merritt and Poff 2010; Shafroth et al. 2017). In the SD reach, although average rates of groundwater recession approached or exceeded thresholds for willow and cottonwood species in many years (Figure 9), anthropogenic water sources sustained limited seedling establishment and survival. These inputs are in part a consequence of the lack of hardened and efficient infrastructure because the valley's irrigation diversions and ditches allow seepage and some down-channel hyporheic flow or vertical connectivity, similar to acequias in northern New Mexico (Fernald et al. 2007). Sporadic inputs in the diverted reach near the SD transect also include excess irrigation water shunted into an overflow channel near the far east end of the transect that is reflected in higher groundwater levels in the east well (SD E) than near the main channel during low-flow periods (Figure 7b). Where secondary channels intercept hyporheic inputs or water from the ditch overflow, they can support dense riparian vegetation; nearly all new recruitment on the SD transect occurs on the floodplain nearest the ditch overflow. Thus, riparian recruitment in the SD reach is spatially restricted, but not precluded, reflecting co-existence of human water use and native riparian needs. Intentional management of irrigation diversions could ensure the continued function and resilience of the GDE riparian system, even with increased aridification. Rohde et al. (2021) caution that riparian systems can become

reliant on water availability due to altered flow regimes, which is not the case in the Cliff-Gila Valley. The gravity-fed irrigation system in the Cliff-Gila Valley physically connects supplemental ditch overflow with river stage in the main channel, reducing its 'artificiality'.

4.4 | Relevance to Colorado River and Other Arid River Systems

The long-term dataset for the Gila River case study demonstrates the resilience of this GDE to multiple cycles of floods and droughts between WY 2011–2021, providing a reference for other rivers in the Colorado River basin and similar arid systems. The Colorado River basin, including the Gila River, will be stressed by increasing aridity projected for the American Southwest (Overpeck and Udall 2020). On the Gila, days of very low flow have already increased, including an unprecedented 21 continuous days of flows below $0.6 \text{ m}^3 \text{ s}^{-1}$ ($20 \text{ ft}^3 \text{ s}^{-1}$) in 2013 (Horner and Dahm 2014). Future climate projections for the Gila River watershed suggest an increase in hydrologic extremes: higher annual temperatures and decreased precipitation during the spring and summer will depress both snowmelt runoff and summer low flows (Garfin et al. 2014; Gutzler 2013). In addition, the North American monsoon may intensify across the southwestern United States, which could result in more large floods during the late summer and autumn (Demaria et al. 2019; Luong et al. 2017).

Anastomosing river systems exhibit interrelated feedbacks between flow, vegetation distribution and river morphology (Henriques et al. 2022) and are, therefore, particularly well-suited to ameliorating natural disturbance regimes like floods and droughts (Entwistle et al. 2018; Polvi and Wohl 2013; Tockner et al. 2000; Wohl et al. 2021). They are also likely more resilient to anthropogenic stressors (Cluer and Thorne 2013; McCluney et al. 2014; Wohl 2024). Before decades of channel straightening, wetland drainage, beaver removal and other river control efforts (Entwistle et al. 2018; Wohl et al. 2021), these systems were far more historically prevalent worldwide than today (Cluer and Thorne 2013; Dépret et al. 2017). In the Cliff-Gila Valley case study, cessation of channelization efforts and changes in grazing management allowed the river to regain access to its floodplain, re-creating a broad network of secondary channels across the river's floodplain. These channels improve access to groundwater, enabling widespread recruitment of native groundwater-dependent riparian vegetation (Figure 6) that effectively attenuates flood forces (Entwistle et al. 2018) and enhances biodiversity, habitat and resist disturbance (Naiman and Décamps 1997).

Another issue that many riparian systems face is invasion of non-native species (Glenn and Nagler 2005; Petrakis et al. 2023). In contrast, our study confirmed a paucity of non-native trees in the Cliff-Gila Valley. In recent years, at perennial Gila sites the timing and gradual rate of groundwater recession (Figures 8 and 9) buffered the annual decline in floodplain groundwater levels that typically occurred from May through much of July (Figure 4). This created advantageous hydrologic conditions that reinforced the natural dominance of native riparian seedlings over non-natives (Busch and Smith 1995) critical for

sustaining native floodplain vegetation over time (Glenn and Nagler 2005; Stromberg, Beauchamp, et al. 2007). Thus, coupled with shallower DTW below the topographic lows of secondary channels, even very low perennial flows enable resilience for native groundwater-dependent riparian forest through extended drought periods.

Conversely, surface water extraction stresses a river's low flow regime; at the SD site on the Gila, these impacts rapidly depressed alluvial groundwater levels. Such groundwater limitations can shift semi-arid riparian systems towards high stress hydrologic conditions that favour non-native species like *Tamarix* (Merritt and Poff 2010; Mortenson and Weisberg 2010). Impacts over time can diminish populations of native foundational species, especially groundwater-dependent cottonwood and willow (Di Tomaso 1998), as throughout much of the Gila River corridor in Arizona, where non-native *Tamarix* dominates (Garssen et al. 2014; Orr et al. 2014; Petrakis et al. 2023). Cohort loss and increased mortality among native trees during extreme or successive years of drought expand the spatial extent of areas suitable for recruitment by non-native species (Glenn and Nagler 2005), reducing available habitat and increasing floodplain temperatures and water loss (Andersen 2015).

4.5 | Importance of Long-Term Field Datasets for Riparian Ecosystems

Long-term ecological datasets can be critical for informing policy and contributing to ecological understanding (Hughes et al. 2017). Techniques using remote sensing have been used to examine temporal and spatial changes of riparian conditions over decadal time spans (Hausner et al. 2018). LiDAR, drones or satellite data can be used to evaluate the dynamics of the system, including groundwater-dependent vegetation responses to floods and summer flow pulses as well as droughts (e.g., Röpke et al. 2017) and anthropogenically modified river flows (Rohde et al. 2021). However, such approaches may not detect smaller areas of vegetation classes, mechanisms of observed changes or dynamics of specific species (Hausner et al. 2018). Further, continuous groundwater data that are difficult to remotely sense provide an invaluable contribution to elucidate functional connectivity between surface water, groundwater and vegetation (Cadot and Wine 2017). On-the-ground monitoring with repeated measurements is an essential dataset for validating approaches such as MRRMaid (<https://www.boisestate.edu/hes/projects/mrrmaid-mesic-resource-restoration-monitoring-aid/>) to understand river and riparian dynamics and trends, particularly considering thresholds associated with decreasing surface and groundwater availability.

5 | Conclusions

The Gila River through the Cliff-Gila Valley in New Mexico is a rare example of a semi-arid river system unaltered by major upstream dams or diversions. Large floods move across the full extent of the broad floodplain, allowing anastomosis to create a complex web of secondary channels. These secondary channels form a crucial functional element of riparian ecosystem

resilience by making groundwater more accessible across the breadth of floodplains, especially to young trees. Thus, they provide conditions that favour successful reproduction by native riparian trees over non-native species. Our analyses over more than a decade for this case study show how topographic complexity created during periodic high flow events interacts with even very low perennial flows to maintain functional connectivity in the Cliff-Gila Valley. While channel dewatering associated with irrigation diversion has immediate and substantial relationships to groundwater levels, even minor amounts of supplemental water can offset these effects, enabling co-existence of human and ecosystem uses of water. This long-term dataset is critical for managing impacts of climate change to maintain resilience in groundwater-dependent riparian systems in the arid Southwest.

Acknowledgements

The authors thank Mary Harner, Mark Briggs, Louis Provencher and Mickey Hazelwood for helpful comments on earlier drafts of the manuscript. Special appreciation is due to Dave Gori for study design and to Dave Propst for his long-term support of the project. Funding was provided in part by the United States Forest Service, New Mexico Department of Game and Fish Contract No. 10-516 0000 00023 and The Nature Conservancy.

Funding

This work was supported by United States Forest Service, New Mexico Department of Game and Fish and The Nature Conservancy.

Data Availability Statement

The data that support the findings of this study are openly available in Hydroshare at <https://doi.org/10.4211/hs.82c2b15884b04af49cff6cdc8c261cb0>.

References

- Andersen, D. C. 2015. "Tree Mortality in Mature Riparian Forest: Implications for Fremont Cottonwood Conservation in the American Southwest." *Western North American Naturalist* 75: 157–169.
- Braatne, J. H., S. B. Rood, and P. E. Heilman. 1995. "Life History, Ecology, and Conservation of Riparian Cottonwoods in North America." In *Biology of Populus and Its Implications for Management and Conservation*, edited by R. F. Stettler, H. D. Bradshaw Jr., P. E. Heilman, and T. M. Hinckley, 57–86. NRC Research Press.
- Busch, D. E., and S. D. Smith. 1995. "Mechanisms Associated With Decline of Woody Species in Riparian Ecosystems of the Southwestern U.S." *Ecological Monographs* 65: 347–370.
- Cadot, D., and M. L. Wine. 2017. "Geomorphology as a First Order Control on the Connectivity of Riparian Ecohydrology." *Geomorphology* 277: 154–170. <https://doi.org/10.1016/j.geomorph.2016.06.022>.
- Capon, S. J., L. E. Chambers, R. Mac Nally, et al. 2013. "Riparian Ecosystems in the 21st Century: Hotspots for Climate Change Adaptation?" *Ecosystems* 16: 359–381. <https://doi.org/10.1007/s10021-013-9656-1>.
- Cluer, B., and C. Thorne. 2013. "A Stream Evolution Model Integrating Habitat and Ecosystem Benefits." *River Research and Applications* 30: 135–154. <https://doi.org/10.1002/rra.2631>.
- Demaria, E. M. C., P. Hazenberg, R. L. Scott, M. B. Meles, M. Nichols, and D. Goodrich. 2019. "Intensification of the North American

- Monsoon Rainfall as Observed From a Long-Term High-Density Gauge Network." *Geophysical Research Letters* 46: 6839–6847. <https://doi.org/10.1029/2019GL082461>.
- Dépret, T., J. Riquier, and H. Piégay. 2017. "Evolution of Abandoned Channels: Insights on Controlling Factors in a Multi-Pressure River System." *Geomorphology* 294: 99–118.
- Di Tomaso, J. M. 1998. "Impact, Biology, and Ecology of Saltcedar (*Tamarix* spp.) in the Southwestern United States." *Weed Technology* 12: 326–336.
- Dufour, S., P. M. Rodriguez-González, and M. Laslier. 2019. "Tracing the Scientific Trajectory of Riparian Vegetation Studies: Main Topics, Approaches, and Needs in a Globally Changing World." *Science of the Total Environment* 653: 1168–1185. <https://doi.org/10.1016/j.scitotenv.2018.10.383>.
- Ellison, A. M., M. S. Bank, B. D. Clinton, et al. 2005. "Loss of Foundation Species: Consequences for the Structure and Dynamics of Forested Ecosystems." *Frontiers in Ecology and the Environment* 3: 479–486.
- Entwistle, N., G. Heritage, and D. Milan. 2018. "Flood Energy Dissipation in Anabranching Channels." *River Research and Applications* 34: 709–720. <https://doi.org/10.1002/rra.3299>.
- Fernald, A. G., T. T. Baker, and S. J. Guldan. 2007. "Hydrologic, Riparian, and Agroecosystem Functions of Traditional Acequia Irrigation Systems." *Journal of Sustainable Agriculture* 30: 147–171. https://doi.org/10.1300/J064v30n02_13.
- Garfin, G., H.-I. Chang, and M. Switanek. 2014. "Chapter 3. Climate and Hydrology of the Upper Gila River Basin." In *Gila River Flow Needs Assessment*, edited by D. Gori, M. S. Cooper, E. S. Soles, et al., 40–79. Nature Conservancy. <https://www.sciencebase.gov/catalog/item/599f217ee4b0e5eb065e3cfd>.
- Garssen, A. G., J. T. A. Verhoeven, and M. B. Soons. 2014. "Effects of Climate-Induced Increases in Summer Drought on Riparian Plant Species: A Meta-Analysis." *Freshwater Biology* 59: 1052–1063.
- Gitlin, A. R., C. M. Stultz, M. A. Bowker, et al. 2006. "Mortality Gradients Within and Among Dominant Plant Populations as Barometers of Ecosystem Change During Extreme Drought." *Conservation Biology* 20: 1477–1486. <https://doi.org/10.1111/j.1523-1739.2006.00424.x>.
- Glenn, E., and P. L. Nagler. 2005. "Comparative Ecophysiology of *Tamarix ramosissima* and Native Trees in Western U.S. Riparian Zones." *Journal of Arid Environments* 61: 419–446.
- Gonzalez, E., V. Martinez-Fernandez, P. B. Shafroth, et al. 2018. "Regeneration of *Salicaceae* Riparian Forests in the Northern Hemisphere: A New Framework and Management Tool." *Journal of Environmental Management* 218: 374–387.
- Gutzler, D. S. 2013. "Streamflow Projections for the Upper Gila River: New Mexico Interstate Stream Commission Report." 27. Accessed July 12, 2023. https://www.ose.state.nm.us/Basins/Colorado/AWSA/Studies/2013_Gutzler_StrmflwProjRpt.pdf.
- Hausner, M. B., J. L. Huntington, C. Nash, et al. 2018. "Assessing the Effectiveness of Riparian Restoration Projects Using Landsat and Precipitation Data From the Cloud-Computing Application ClimateEngine.Org." *Ecological Engineering* 120: 432–440. <https://doi.org/10.1016/j.ecoleng.2018.06.024>.
- Hawley, J. W., B. J. Hibbs, J. F. Kennedy, et al. 2000. Trans-International Boundary Aquifers in Southwest New Mexico." Technical Completion Report Prepared for U.S. Environmental Protection Agency—Region 6 and the International Boundary and Water Commission—U.S. Section. March 2000.
- Henriques, M., T. R. McVicar, K. L. Holland, and E. Daly. 2022. "Riparian Vegetation and Geomorphological Interactions in Anabranching Rivers: A Global Review." *Ecohydrology* 15: e2370. <https://doi.org/10.1002/eco2370>.
- Horner, M., and C. N. Dahm. 2014. "Ecohydrology and Recent Climatology of the Gila River. Chapter 2." In *Gila River Flow Needs Assessment*, edited by D. Gori, M. S. Cooper, E. S. Soles, et al., 4–39. Nature Conservancy. <https://www.sciencebase.gov/catalog/item/599f217ee4b0e5eb065e3cfd>.
- Horton, J. L., and J. L. Clark. 2001. "Water Table Decline Alters Growth and Survival of *Salix gooddingii* and *Tamarix chinensis* Seedlings." *Forest Ecology and Management* 140: 239–247.
- Horton, J. L., T. E. Kolb, and S. C. Hart. 2001. "Responses of Riparian Trees to Inter-Annual Variation in Ground Water Depth in a Semi-Arid River Basin." *Plant, Cell & Environment* 24: 293–304.
- Hughes, B. B., R. Beas-Luna, A. K. Barner, et al. 2017. "Long-Term Studies Contribute Disproportionately to Ecology and Policy." *Bioscience* 67: 271–281. <https://doi.org/10.1093/biosc/btw185>.
- Kauffman, J. B., and W. C. Krueger. 1984. "Livestock Impacts on Riparian Ecosystems and Streamside Management Implications: A Review." *Journal of Range Management* 37: 430–438.
- Kondolf, G. M. 2011. "Setting Goals in River Restoration: When and Where Can the River 'Heal Itself'?" In *Geophysical Monograph*, edited by A. Simon, S. J. Bennett, and J. M. Castro, vol. 194, 29–43. American Geophysical Union.
- Kumar, S., T. J. Stohlgren, and G. W. Chong. 2006. "Spatial Heterogeneity Influences Native and Nonnative Plant Species Richness." *Ecology* 87: 3186–3199.
- Leenhouts, J. M., J. C. Stromberg, and R. L. Scott. 2006. *Hydrologic Requirements of and Consumptive Groundwater Use by Riparian Vegetation Along the San Pedro River, Arizona. U.S Geological Survey Scientific Investigations Report 2005–5163*, 154. U.S Geological Survey.
- Lite, S. J., and J. C. Stromberg. 2005. "Surface Water and Ground-Water Thresholds for Maintaining *Populus-Salix* Forests, San Pedro River, Arizona." *Biological Conservation* 125: 153–167.
- Luong, T. M., C. L. Castro, H.-I. Chang, T. Lahmers, D. K. Adams, and C. A. Ochoa-Moya. 2017. "The More Extreme Nature of North American Monsoon Precipitation in the Southwestern United States as Revealed by a Historical Climatology of Simulated Severe Weather Events." *Journal of Applied Meteorology and Climatology* 56: 2509–2529. <https://doi.org/10.1175/AMC-D-16-0358.1>.
- Lytle, D. A., and D. M. Merritt. 2004. "Hydrologic Regimes and Riparian Forests: A Structured Population Model for Cottonwood." *Ecology* 85: 2493–2503.
- Mahoney, J. M., and S. B. Rood. 1998. "Streamflow Requirements for Cottonwood Seedling Recruitment—An Integrative Model." *Wetlands* 18: 634–645.
- Mayes, M., K. K. Caylor, M. B. Singer, J. C. Stella, D. Roberts, and P. Nagler. 2020. "Climate Sensitivity of Water Use by Riparian Woodlands at Landscape Scales." *Hydrological Processes* 34: 4884–4903. <https://doi.org/10.1002/hyp.13942>.
- McCluney, K. E., N. L. Poff, M. A. Palmer, et al. 2014. "Riverine Macrosystems Ecology: Sensitivity, Resistance, and Resilience of Whole River Basins With Human Alterations." *Frontiers in Ecology and the Environment* 12: 48–58. <https://doi.org/10.1890/120367>.
- Merritt, D. M., and H. L. Bateman. 2012. "Linking Stream Flow and Groundwater to Avian Habitat in a Desert Riparian System." *Ecological Applications* 22: 1973–1988.
- Merritt, D. M., and N. L. Poff. 2010. "Shifting Dominance of Riparian *Populus* and *Tamarix* Along Gradients of Flow Alteration in Western North American Rivers." *Ecological Applications* 20: 135–152.
- Mortenson, S. G., and P. J. Weisberg. 2010. "Does River Regulation Increase the Dominance of Invasive Woody Species in Riparian Landscapes?" *Global Ecology and Biogeography* 19: 562–574.

- Naiman, R. J., and H. Décamps. 1997. "The Ecology of Interfaces: Riparian Zones." *Annual Review of Ecology and Systematics* 28: 621–658.
- NRC. 2002. *Riparian Areas: Functions and Strategies for Management*. National Academies Press. <https://doi.org/10.17226/10327>.
- Office of the State Engineer. 2022. "New Mexico Interstate Stream Commission, Gila Basin Ditch Diversions." https://www.ose.state.nm.us/Basins/Colorado/isc_Gila.php.
- Orr, B. K., G. T. Leverich, Z. E. Diggory, T. L. Dudley, J. R. Hatten, and K. R. Hultine. 2014. *Riparian Restoration Framework for the Upper Gila River, Arizona*. Gila Watershed Partnership of Arizona.
- Overpeck, J. T., and B. Udall. 2020. "Climate Change and the Aridification of North America." *Proceedings of the National Academy of Sciences of the United States of America* 117: 11856–11858.
- Palmer, M. A., D. P. Lettenmaier, N. L. Poff, S. L. Postel, B. Richter, and R. Warner. 2009. "Climate Change and River Ecosystems: Protection and Adaptation Options." *Environmental Management* 44: 1053–1068.
- Patten, D. T. 1998. "Riparian Ecosystems of Semi-Arid North America: Diversity and Human Impacts." *Wetlands* 18: 498–512.
- Petrakis, R. E., L. M. Norman, and B. R. Middleton. 2023. "Riparian Vegetation Response Amid Variable Climate Conditions Across the Upper Gila River Watershed: Informing Tribal Restoration Priorities." *Frontiers in Environmental Science* 11: 1179328. <https://doi.org/10.3389/fenvs.2023.1179328>.
- Polvi, L. E., and E. Wohl. 2013. "Biotic Drivers of Stream Planform: Implications for Understanding the Past and Restoring the Future." *Bioscience* 63: 439–452.
- Powers, P. D., M. Helstab, and S. L. Niezgod. 2019. "A Process-Based Approach to Restoring Depositional River Valleys to Stage 0, an Anastomosing Channel Network." *River Research and Applications* 35: 3–13. <https://doi.org/10.1002/rra.3378>.
- Propst, D. L. 2019. *River Flow, Drought, Flood, and Wildfire: Response of Gila River Fish Assemblage*, 27. Nature Conservancy.
- Räpple, B., H. Piégay, J. C. Stella, and D. Mercier. 2017. "What Drives Riparian Vegetation Encroachment in Braided River Channels at Patch to Reach Scales? Insights From Annual Airborne Surveys (Drôme River, SE France, 2005–2011)." *Ecohydrology* 10: e1886. <https://doi.org/10.1002/eco.1886>.
- Rohde, M. M., J. C. Stella, D. A. Roberts, and M. B. Singer. 2021. "Groundwater Dependence of Riparian Woodlands and the Disrupting Effect of Anthropogenically Altered Streamflow." *Proceedings of the National Academy of Sciences* 118: e2026453118. <https://doi.org/10.1073/pnas.2026453118>.
- Rood, S. B., J. H. Braatne, and L. A. Goater. 2010. "Responses of Obligate Versus Facultative Riparian Shrubs Following River Damming." *River Research and Applications* 26: 102–117.
- Rood, S. B., J. H. Braatne, and F. M. R. Hughes. 2003. "Ecophysiology of Riparian Cottonwoods: Stream Flow Dependency, Water Relations and Restoration." *Tree Physiology* 23: 1113–1124.
- Rood, S. B., C. R. Gourley, E. M. Ammon, et al. 2003. "Flows for Floodplain Forests: A Successful Riparian Restoration." *Bioscience* 53: 647–656.
- Sabo, J. L., R. Sponseller, M. Dixon, et al. 2005. "Riparian Zones Increase Regional Species Richness by Harboring Different, Not More, Species." *Ecology* 86: 56–62.
- Schumm, S. A. 1985. "Patterns of Alluvial Rivers." *Annual Review of Earth and Planetary Sciences* 13: 5–27.
- Scott, M. L., P. B. Shafroth, and G. T. Auble. 1996. "Responses of Riparian Cottonwoods to Alluvial Water Table Declines." *Environmental Management* 23: 347–358.
- Shafroth, P. B., K. J. Schlatter, M. Gomez-Sapiens, et al. 2017. "A Large-Scale Environmental Flow Experiment for Riparian Restoration in the Colorado River Delta." *Ecological Engineering* 106: 645–660.
- Shafroth, P. B., J. C. Stromberg, and D. T. Patten. 2000. "Woody Riparian Vegetation Response to Different Alluvial Water Table Regimes." *Western North American Naturalist* 60: 66–76.
- Sher, A. A., D. L. Marshall, and S. A. Gilbert. 2000. "Competition Between Native *Populus deltoides* and Invasive *Tamarix ramosissima* and the Implications for Reestablishing Flooding Disturbance." *Conservation Biology* 14: 1744–1754.
- Sher, A. A., D. L. Marshall, and J. P. Taylor. 2002. "Establishment Patterns of Native *Populus* and *Salix* in the Presence of Invasive Nonnative *Tamarix*." *Ecological Applications* 12: 760–772.
- Skidmore, P., and J. Wheaton. 2022. "Riverscapes as Natural Infrastructure: Meeting Challenges of Climate Adaptation and Ecosystem Restoration." *Anthropocene* 38: 100334. <https://doi.org/10.1016/j.ancene.2022.100334>.
- Smith, S. D., D. A. Devitt, A. Sala, J. R. Cleverly, and D. E. Busch. 1998. "Water Relations of Riparian Plants From Warm Desert Regions." *Wetlands* 18: 687–696.
- Soles, E. S. 2003. "Where the River Meets the Ditch: Human and Natural Impacts on the Gila River, New Mexico, 1880–2000." MS thesis, Northern Arizona University, 166.
- Soles, E. S. 2014. "Chapter 4: Fluvial Geomorphology of the Gila River, Cliff–Gila Valley, NM." In *Gila River Flow Needs Assessment*, edited by D. Gori, M. S. Cooper, E. S. Soles, et al., 80–94. Nature Conservancy. <https://www.sciencebase.gov/catalog/item/599f217ee4b0e5eb065e3cfd>.
- Stella, J. C., and J. J. Battles. 2010. "How Do Riparian Woody Seedlings Survive Seasonal Drought?" *Oecologia* 164: 579–590.
- Stella, J. C., J. J. Battles, J. R. McBride, and B. K. Orr. 2010. "Riparian Seedling Mortality From Simulated Water Table Recession, and the Design of Sustainable Flow Regimes on Regulated Rivers." *Restoration Ecology* 18: 284–294.
- Stromberg, J. C. 1997. "Growth and Survivorship of Fremont Cottonwood, Goodding Willow, and Salt Cedar Seedlings After Large Floods in Central Arizona." *Great Basin Naturalist* 47: 196–208.
- Stromberg, J. C., V. B. Beauchamp, M. D. Dixon, S. J. Lite, and C. Paradzick. 2007. "Importance of Low-Flow and High-Flow Characteristics to Restoration of Riparian Vegetation Along Rivers in Arid South-Western United States." *Freshwater Biology* 52: 651–679.
- Stromberg, J. C., S. J. Lite, R. Marler, et al. 2007. "Altered Stream-Flow Regimes and Invasive Plant Species: The *Tamarix* Case." *Global Ecology and Biogeography* 18: 381–393.
- Stromberg, J. C., R. Tiller, and B. Richter. 1996. "Effects of Groundwater Decline on Riparian Vegetation of Semiarid Regions: The San Pedro, Arizona." *Ecological Applications* 6: 113–131.
- Tetra Tech, Inc. 2010. "Gila River 2010 Piezometers Memo." Unpublished Draft Technical Memorandum to New Mexico Interstate Stream Commission, June 15, 2010.
- Tockner, K., F. Malard, and J. V. Ward. 2000. "An Extension of the Flood Pulse Concept." *Hydrological Processes* 14: 2861–2883.
- Udall, B., and J. Overpeck. 2017. "The Twenty-First Century Colorado River Hot Drought and Implications for the Future." *Water Resources Research* 53: 2404–2418. <https://doi.org/10.1002/2016WR019638>.
- United States Geological Survey. 2022a. "National Water Information System, USGS 09430500 Gila River Near Gila, NM." <https://waterdata.usgs.gov/monitoring-location/09430500/>.
- United States Geological Survey. 2022b. "National Water Information System, USGS 09430600 Mogollon Creek Near Cliff, NM." <https://waterdata.usgs.gov/monitoring-location/09430600/>.

Van der Nat, D., K. Tockner, P. J. Edwards, J. V. Ward, and A. M. Gurnell. 2003. "Habitat Change in Braided Flood Plains (Tagliamento, NE-Italy)." *Freshwater Biology* 48: 1799–1812.

Webb, A. D., D. A. Falk, and D. M. Finch. 2019. *Fire Ecology and Management in Lowland Riparian Ecosystems of the Southwestern United States and Northern Mexico. Gen. Tech. Rep. RMRS-GTR-401*, 132. USDA Forest Service, Rocky Mountain Research Station.

Western Regional Climate Center. 2023. "Monthly Climate Summaries for Cliff 11 SE, New Mexico COOP and Gila Hot Springs, New Mexico COOP Stations." <https://wrcc.dri.edu/summary/Climsmnm.html>.

Whited, D. C., M. S. Lorang, M. J. Harner, F. R. Hauer, J. S. Kimball, and J. A. Stanford. 2007. "Climate, Hydrologic Disturbance, and Succession: Drivers of Floodplain Pattern." *Ecology* 88: 940–953.

Whitney, K. M., E. R. Vivoni, T. J. Bohn, et al. 2023. "Spatial Attribution of Declining Colorado River Streamflow Under Future Warming." *Journal of Hydrology* 617: 129125. <https://doi.org/10.1016/j.jhydrol.2023.129125>.

Williams, A. P., B. I. Cook, and J. E. Smerdon. 2022. "Rapid Intensification of the Emerging Southwestern North American Megadrought in 2020–2021." *Nature Climate Change* 12: 232–234. <https://doi.org/10.1038/s41558-022-01290-z>.

Wittler, R. J., and D. R. Levish. 2004. *Upper Gila River Fluvial Geomorphology Study, Final Report, New Mexico*, 62. U.S. Bureau of Reclamation.

Wohl, E. 2024. "Resilience in River Corridors: How Much Do We Need?" *Perspectives of Earth and Space Scientists* 5: e2023CN000226. <https://doi.org/10.1029/2023CN000226>.

Wohl, E., J. Castro, B. Cluer, et al. 2021. "Rediscovering, Reevaluating, and Restoring Lost River-Wetland Corridors." *Frontiers in Earth Science* 9: 653623. <https://doi.org/10.3389/feart.2021.653623>.

Supporting Information

Additional supporting information can be found online in the Supporting Information section. **Data S1:** hyp70406-sup-0001-Supinfo.docx.